ELSEVIER

Biochimica et Biophysica Acta 1238 (1995) 86–90

BBA Biochimica et Biophysica Acta

Rapid Report

Real-time analysis of liposomal trafficking in tumor-bearing mice by use of positron emission tomography

Naoto Oku [a,*], Yoshihiro Tokudome [a], Hideo Tsukada [b], Shoji Okada [a]

[a] *Department of Radiobiochemistry, School of Pharmaceutical Sciences, University of Shizuoka, Yada, Shizuoka 422, Japan*

[b] *Center Research Laboratory, Hamamatsu Photonics and Subfemtomole Biorecognition Project, Research Development Corporation of Japan, Hamakita, Shizuoka, Japan*

Received 6 February 1995; revised 29 March 1995; accepted 29 March 1995

Abstract

Long-circulating liposomes are known to accumulate passively in tumor tissues of tumor-bearing animals. To evaluate the in vivo behavior of such liposomes, we investigated the real-time liposomal trafficking by a non-invasive method using positron emission tomography (PET). Liposomes composed of dipalmitoylphosphatidylcholine, cholesterol, and palmityl-D-glucuronide (PGlcUA) in a molar ratio of 4:4:1 were prepared in the presence of 2-[^{18}F]fluoro-2-deoxyglucose ([2-^{18}F]FDG). [2-^{18}F]FDG-labeled liposomes sized by extrusion through a filter with various-sized pores were administered to mice bearing Meth A sarcoma, and a PET scan was performed for 120 min. Small-sized, long-circulating liposomes (100 nm in diameter) constructed with PGlcUA tended to accumulate in the tumor tissues. On the contrary, control liposomes (100 nm in diameter) containing dipalmitoylphosphatidylglycerol instead of PGlcUA accumulated in the liver. Large-sized PGlcUA-containing liposomes (> 300 nm) also accumulated in the liver, as well as in the spleen. Time–activity curves indicated that the small long-circulating liposomes (< 200 nm) transiently accumulated in the liver right after the injection but that the accumulation there decreased time-dependently. These data suggest that, although the majority of small long-circulating liposomes remain in the bloodstream, some extravasate once into the interstitial spaces in the liver re-enter the bloodstream again, and finally accumulate in the tumor tissues. This PET technique might be useful for studying real-time liposomal trafficking and for tumor imaging.

Keywords: Liposome; Positron emission tomography (PET); Long-circulating liposome; Tumor imaging

Liposomes can be used as ideal drug carriers, especially for anticancer agents, since they can encapsulate and deliver large amounts of agents to the target organs, and can reduce the rapid excretion of these agents 1 [1–4]. Conventional liposomes, however, have a limitation for cancer therapy, since they tend to be trapped by the reticuloendothelial system (RES) such as in the liver. Recently it was shown that reduced RES uptake was achieved by the modification of liposomes with monosialoganglioside GM1 [5,6] or polyethyleneglycol (PEG) [7–11], although GM1 modification was revealed to be effective only in mice and not in rats [12] or rabbits [13].

These long-circulating liposomes showed further advantage for cancer therapy due to passive accumulation in tumor tissues, since the vasculature in the tumor tissues is leaky enough for extravasation of small-sized liposomes. We previously reported that the liposomes modified with a glucuronic acid derivative, palmityl-D-glucuronide (PGlcUA), had a longer circulation time in the bloodstream of rats [14] and mice [15] than conventional liposomes containing DPPG, and accumulated in the tumor tissue of tumor-bearing mice [15]. In this present study utilizing positron emission tomography (PET), we investigated the real-time biodistribution change of conventional and long-circulating liposomes having an encapsulated positron emitter. This technique is also applicable for tumor imaging.

Dipalmitoylphosphatidylcholine (DPPC), dipalmitoylphosphatidylglycerol (DPPG), and palmityl-D-glucuronide (PGlcUA) were kindly donated by Dr. Yukihiro Namba at Nippon Fine Chemical Co. Cholesterol was purchased from Sigma (St. Louis, MO), and reduced Triton X-100 was from Aldrich. Fetal bovine serum (FBS) was obtained from Hazleton. [^{14}C]FDG was purchased from Amersham.

Liposomes were prepared as follows: DPPC, choles-

* Corresponding author. Fax: +81 54 2645705.

SSDI 0005-2736(95)00106-9

terol, and PGlcUA or DPPG (4:4:1, molar ratio) dissolved in chloroform were dried under reduced pressure and stored in vacuo for at least 1 h. Liposomes were produced by hydration of the thin lipid film with 1.0 ml of 0.45 M sodium gluconate. This liposomal solution was mixed with 2.0 ml of [2-^{18}F]FDG solution and freeze-thawed for three cycles using liquid nitrogen to encapsulate the radioactive chemical into the liposomes. Then the liposomes were extruded three times through a polycarbonate membrane filter. Thus obtained sized liposomes were diluted with saline, centrifuged at $320\,000 \times g$ for 20 min in order to remove the untrapped [2-^{18}F]FDG, and resuspended in saline. The encapsulation efficiency was 10–15%, depending on the liposomal sizes.

PET analysis of liposomal trafficking in tumor-bearing mice was performed as follows: Seven-week-old Balb/c male mice (Japan SLC Inc.) were subcutaneously inoculated into the right posterior flank with 10^6 Meth A sarcoma cells. Seventeen days after tumor implantation, the mice weighing 25–30 g were anesthetized with sodium pentobarbital and injected into a tail vein with positron-labeled liposomes. Tumors having grown for the same length of time in mice injected with liposomes were weighed and observed to be between 0.6 and 1.9 g. The dose was 9 μmol as total lipids, and about 1.85 MBq. The emission scan was started immediately after injection and performed for 120 min with an animal PET camera (Hamamatsu Photonics, HSR-2000) having an effective slice aperture of 3.25 mm and resolution of less than 3 mm [16]. Scan frame intervals were 2 min during first 60 min and 5 min during 60 to 120 min. Before injection of the liposomes, transmission scans were obtained by use of an 18.5 MBq ^{68}Ge/Ga ring source for attenuation correction. The radioactivity in the form of coincidence gamma photons was measured and converted to Bq/cm^3 of tissue volume by calibration after correction for decay and attenuation. A time–activity curve was obtained from the mean pixel radioactivity in the region of interest (ROI) of the PET images. The result of the PET experiment presented in this paper is a typical one obtained from a single scan, and similar results were obtained in another repeated experiment.

Prior to the PET study, liposomal stability in the serum was evaluated by the leakage of [^{14}C]FDG from liposomes. Liposomes encapsulating [^{14}C]FDG were prepared by the same procedure as used for the preparation of [2-^{18}F]FDG-labeled liposomes. Then the liposomes were incubated in PBS or 90% FBS at 37°C, and aliquots were collected at specific times and centrifuged. The radioactivity in the supernatant was measured with a liquid scintillation counter (Aloka, LSC3100). Only less than 10% of FDG was released from all kinds of liposomes tested after a 2-h incubation both in the presence and absence of serum, suggesting that the biodistribution of [2-^{18}F]FDG reflects that of liposomes in vivo.

Then the PET analysis of liposomal trafficking was performed. Fig. 1 shows the biodistribution of PGlcUA-liposomes in an individual mouse. PET images were composed by the summation of the first 30 min of accumulation, and corresponding magnetic resonance images taken of another mouse similarly settled. The images in the figure show the coronal planes ordered from the tail side (upper left) to the head side (lower right), and indicate the positions of the spleen (right side of the images in 4th and 5th slices), liver (7th and 8th slices), lungs (10th to 12th slices) and heart (11th slice). Intense accumulation of radioactivity shown in the 11th slice of PET images indicates the liposomes in the blood in heart, suggesting the high retention of the liposomes in the blood pool. The result was confirmed by direct counting of the heart and blood radioactivities after killing the animal (data not shown). Fig. 2 shows the accumulation of PGlcUA liposomes of various sizes as well as that of 100-nm conventional liposomes during the 90 to 120 min period after injection of liposomes. Liposomal sizes tested were determined by dynamic laser light scattering (Nicomp Model 370). The observed diameters of 100-nm, 200-nm, 300-nm, and 400-nm liposomes were 111 nm, 198 nm, 280 nm and 420 nm, respectively. In the case of PGlcUA-liposomes, liver and spleen accumulations decreased with decreasing liposomal sizes, although splenic accumulation was greater compared with the hepatic for all sizes. On the contrary, accumulation in the tumor was increased by decreasing the sizes, and the highest accumulation was obtained when the 100-nm PGlcUA-liposomes were injected. Conventional liposomes containing DPPG instead of PGlcUA accumulated intensely in liver, although the size of the liposomes was only 100 nm. These data are consistent with previous observations that 100-nm PGlcUA-liposomes can avoid liver-trapping and accumulate in tumor tissue effectively [15]. Accumulation of any kind of liposomes was not observed in lungs, heart, kidneys, and the residual tissues by PET imaging; i.e., it only occurred in the RES and tumor tissues.

Fig. 3 shows the time–activity curves of liposomal accumulation in liver, spleen, and tumor. The trafficking of small-sized, long-circulating liposomes of 200 nm or less was apparently different from that of larger liposomes. Hepatic and splenic accumulation of these liposomes decreased time-dependently. Interestingly, these liposomes were found in the liver at a rather high level immediately after injection compared with larger liposomes. The initial accumulation of these liposomes in the liver might be due to extravasation of these liposomes into interstitial spaces of the liver; those liposomes would then re-enter the bloodstream. Such observation could be obtained only by the non-invasive real-time analysis. On the contrary, large liposomes of 300 nm or more accumulated in the liver time-dependently, suggesting the RES-trapping of these liposomes. Splenic uptake of the liposomes was also size-dependent, and reached a plateau at approx. 20 min.

Tumor accumulation was also size dependent, but the

Fig. 1. Biodistribution of [2-^{18}F]FDG-labeled PGlcUA-liposomes imaged by PET. PGlcUA-liposomes composed of DPPC, cholesterol, and PGlcUA (4:4:1, molar ratio) were prepared in the presence of [2-^{18}F]FDG and extruded through a 100-nm pore filter as described in the text. The [2-^{18}F]FDG-labeled liposomes were injected intravenously into a 7-week-old BALB/c male mouse, and the emission scan was performed as described in the text. The mouse was fixed as abdomen side up. Coronal PET images (left panel) and corresponding MR images (right) are shown with a slice aperture of 3.25 mm, from the tail side (upper left) to the head side (lower right).

Fig. 2. Biodistribution of PGlcUA-liposomes of various sizes imaged by PET. [2-^{18}F]FDG-labeled PGlcUA-liposomes of various sizes composed of DPPC, cholesterol, and PGlcUA (4:4:1, molar ratio), and 100-nm DPPG-liposomes composed of DPPC, cholesterol, and DPPG (4:4:1, molar ratio), were prepared as described in the text. These liposomes were injected into BALB/c male mice bearing Meth A sarcoma, and on emission scan was performed as described in the text. PET images show the accumulation of liposomes during the 90 to 120 min period after the injection. Tumor is located at the left side of the liver shown in the upper panel images, and the spleen, at the right side of the lower images.

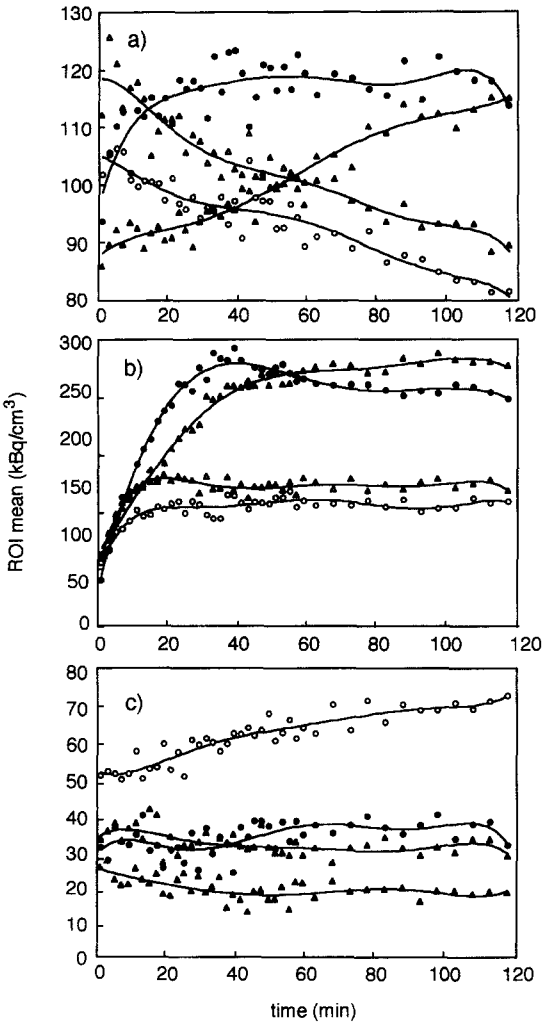

Fig. 3. Real-time changes in PGlcUA-liposomal biodistribution determined by PET. Time–activity curves of ^{18}F in liver (a), spleen (b), and tumor (c) were obtained as described in the text after injection of 100-nm (○), 200-nm (△), 300-nm (●), and 400-nm (▲) liposomes.

critical size might be less than 200 nm, since only the 100-nm long-circulating liposomes accumulated to become 2-to 4-fold over the level of the other three sizes of liposomes at 2 h after the start of incubation. These results indicate the fenestrae of the endothelium in tumor tissues are smaller than those of the sinusoidal endothelium in the liver.

Generally, liposomes are recognized and trapped by the RES, and suppression of this recognition results in prolongation of liposomal half-life in the bloodstream. Long-circulating liposomes tend to accumulate in tumor tissues by passive targeting. For tumor imaging and therapy, it is preferable that the agents accumulate in the tumor and not in other tissues. Thus long-circulating liposomes may provide a useful tool for imaging [17,18] and therapy [19–21] of tumors. Liu and co-workers investigated the biodistribution of another kind of long-circulating liposomes of various sizes, although their method was invasive [22]. They also observed that 100–200-nm liposomes were favorable for tumor targeting, although smaller liposomes, those less than 70 nm, accumulated in the liver. Such smaller vesicles might be trapped by RES cells, namely, Kupffer cells, in the liver, due to decreased long-circulating capability as in the case of PEG-liposomes [23].

This non-invasive method to determine real-time liposomal trafficking in vivo is beneficial for obtaining information about liposomal drug disposition, and for preparing appropriate formulations of the drug carriers. Furthermore, since long-circulating liposomes tend to accumulate in the tumor, they might be useful for diagnostic tumor imaging.

This work was supported in part by a Grant-in-Aid for Scientific Research from the Ministry of Education, Science, and Culture of Japan.

References

[1] Rolland, A., ed. (1993) Pharmaceutical particulate carriers: Therapeutic applications, Marcel Dekker, New York.
[2] Namba, Y. and Oku, N. (1993) J. Bioact. Compat. Polym. 8, 158–177.
[3] Gregoriadis, G., ed. (1992) Liposome technology, 2nd Edn., CRC Press, Boca Raton, FL.
[4] Hagiwara, A., Takahashi, T. and Oku, N. (1989) CRC Crit. Rev. Oncol. Hematol. 9, 319–350.
[5] Allen, T.M. and Chonn, A. (1987) FEBS Lett. 223, 42–46.
[6] Gabizon, A. and Papahadjopoulos, D. (1988) Proc. Natl. Acad. Sci. USA 85, 6949–6953.
[7] Blume, G. and Cevc, G. (1990) Biochim. Biophys. Acta 1029, 91–97.
[8] Klibanov, A.L., Maruyama, K., Torchilin, V.P. and Huang, L. (1990) FEBS Lett. 268, 235–237.
[9] Allen, T.M., Austin, G.A., Chonn, A., Lin, L. and Lee, K.C. (1991) Biochim. Biophys. Acta 1061, 56–64.
[10] Senior, J., Delgado, C., Fisher, D., Tilcock, C. and Gregoriadis, G. (1991) Biochim. Biophys. Acta 1062, 77–82.
[11] Klibanov, A.L., Maruyama, K., Beckerleg, A.M., Torchilin, V.P. and Huang, L. (1991) Biochim. Biophys. Acta 1062, 142–148.
[12] Yamauchi, H., Yano, T., Kato, T., Tanaka, I., Nakabayashi, S., Higashi, K., Miyoshi, S. and Yamada, H. (1995) Int. J. Pharm. 113, 141–148.
[13] Tilcock, C., Ahkong, Q.F. and Fisher, D. (1993) Biochim. Biophys. Acta 1148, 77–84.
[14] Namba, Y., Sakakibara, T., Masada, M., Ito, F. and Oku, N. (1990) Chem. Pharm. Bull. 38, 1663–1666.
[15] Oku, N., Namba, Y. and Okada, S. (1992) Biochim. Biophys. Acta 1126, 255–260.
[16] Watanabe, M., Uchida, H., Okada, H., Shimizu, K., Satoh, N., Ohmura, T., Yamashita, T. and Tanaka, E. (1992) IEEE Trans. Med. Imaging 11, 577–580.
[17] Oku, N., Namba, Y., Takeda, A. and Okada, S. (1993) Nucl. Med. Biol. 20, 407–412.
[18] Woodle, M.C. (1993) Nucl. Med. Biol. 20, 149–155.
[19] Vaage, J., Donovan, D., Mayhew, E., Uster, P. and Woodle, M. (1993) Int. J. Cancer 54, 959–964.
[20] Oku, N., Doi, K., Namba, Y. and Okada, S. (1994) Int. J. Cancer 58, 415–419.
[21] Vaage, J., Barbera-Guillem, E., Abra, R., Huang, A. and Working, P. (1994) Cancer 73, 1478–1484.
[22] Liu, D., Mori, A. and Huang, L. (1992) Biochim. Biophys. Acta 1104, 95–101.
[23] Litzinger, D.C., Buiting, A.M.J., Van Rooijen, N. and Huang, L. (1994) Biochim. Biophys. Acta 1190, 99–107.